Poly(rC)-binding protein 1 limits hepatitis C virus assembly and egress

Sophie E. Cousineau[1] and Selena M. Sagan[1,2]#

[1]Department of Microbiology & Immunology, McGill University, Montreal, QC, Canada

[2]Department of Biochemistry, McGill University, Montreal, QC, Canada

#Corresponding Author: Dr. Selena Sagan, McGill University, 3655 Promenade Sir William Osler, Room 805, Montréal, QC, H3G 1Y6; email: selena.sagan@mcgill.ca

Keywords: Hepatitis C virus (HCV), poly(rC)-binding protein 1 (PCBP1), hnRNP E1, assembly, egress

Running title: PCBP1 limits HCV assembly and egress

ABSTRACT

The hepatitis C virus (HCV) co-opts a number of cellular elements – including proteins, lipids, and microRNAs – to complete its viral life cycle. The cellular RNA-binding protein poly(rC)-binding protein 1 (PCBP1) had previously been reported to bind the HCV genome 5′ untranslated region (UTR), but its importance in the viral life cycle has remained unclear. Herein, we aimed to clarify the role of PCBP1 in the HCV life cycle. Using the HCV cell culture (HCVcc) system, we found that endogenous PCBP1 knockdown decreased viral RNA accumulation yet increased extracellular virus titers. To dissect PCBP1's specific role in the viral life cycle, we carried out assays for viral entry, translation, genome stability, RNA replication, virion assembly and egress. We found that PCBP1 did not affect viral entry, translation, RNA stability, or RNA replication in the absence of efficient virion assembly. To specifically examine virion assembly and egress, we inhibited viral RNA replication with an RNA-dependent RNA polymerase inhibitor and tracked both intracellular and extracellular viral titers over time. We found that when viral RNA accumulation was inhibited, knockdown of PCBP1 still resulted in an overall increase in HCV particle secretion. We therefore propose a model where endogenous PCBP1 limits virion assembly and egress, thereby indirectly enhancing viral RNA accumulation in infected cells. This model furthers our understanding of how cellular RNA-binding proteins modulate HCV genomic RNA utilization during the viral life cycle.

IMPORTANCE

Hepatitis C virus (HCV) is a positive-sense RNA virus, and as such, its genome must be a template for multiple mutually exclusive steps of the viral life cycle, namely translation, RNA replication, and virion assembly. However, the mechanism(s) that regulate how the viral genome

38 is used throughout the viral life cycle still remain unclear. A cellular RNA-binding protein –
39 PCBP1 – had previously been reported to bind the HCV genome, but its precise role in the viral
40 life cycle was not known. In this study, we found that depleting PCBP1 decreased viral RNA
41 accumulation but increased virus secretion. We ruled out a role for PCBP1 in virus entry,
42 translation, genome stability or RNA replication, and demonstrate that PCBP1 knockdown
43 enhances virus secretion when RNA replication is inhibited. We conclude that PCBP1 normally
44 prevents virus assembly and egress, which allows more of the viral genomic RNA to be available
45 for translation and viral RNA replication.

INTRODUCTION

The hepatitis C virus (HCV) is an enveloped virus of the *Flaviviridae* family (genus: hepacivirus) that typically causes a persistent liver infection (1). Its ~9.6 kb single-stranded, positive-sense RNA genome contains a single open reading frame flanked by 5′ and 3′ untranslated regions (UTR). A highly structured, type 3 internal ribosomal entry site (IRES) in the 5′ UTR drives the translation of the viral polyprotein, which is subsequently processed into 10 mature viral proteins: 3 structural proteins (core, E1 and E2 glycoproteins), and 7 nonstructural (NS) proteins (p7, NS2, NS3, NS4A, NS4B, NS5A and NS5B) (2, 3). While the structural proteins form the nucleocapsid and viral envelope, the NS3-5B form the viral replicase, required for viral RNA replication (4). The p7, NS2, NS3 and NS5A proteins have also been implicated in viral genome packaging and the assembly of new virion particles (5-8). As a positive-sense RNA virus, the HCV genome itself must serve as a template for viral translation, genome replication, and packaging; however, the mechanisms that determine which process each viral RNA is engaged in at any given time have not been defined. Due to their limited coding capacity, viruses are highly dependent on the molecular machinery of the host cell; thus, it is likely that cellular components participate in regulation of the viral RNA during the HCV life cycle. While a number of cellular proteins and RNAs have been shown to interact with the HCV genome, their precise role(s) in the viral life cycle have yet to be defined.

The poly(rC)-binding protein 1 (PCBP1) is one of the three most abundant cellular RNA-binding proteins with a strong affinity for poly(rC), along with its paralogs hnRNP K and PCBP2 (9). These multifunctional proteins can regulate translation and enhance the stability of their cellular mRNA targets, which they interact with through their hnRNP K homologous (KH) domains (10). Notably, all three paralogs have been reported to bind to the HCV 5′ UTR (11-

13). However, the degree to which each protein has been studied in the context of HCV infection varies significantly – while hnRNP K and PCBP2 have been fairly extensively studied and reported to play markedly different roles in the viral life cycle, the role of PCBP1 in the HCV life cycle has not been investigated in detail (14, 15). Beyond its interactions with the 5′ UTR, previous reports suggested that PCBP1 was not necessary for HCV IRES-mediated translation, but that knockdown of PCBP1 decreases HCV RNA accumulation during infection (16, 17).

Herein, we sought to clarify the role of PCBP1 in the HCV life cycle. Using a cell culture-adapted strain of HCV, we found that PCBP1 knockdown decreased viral RNA accumulation, yet led to an increase in virus secretion. By examining individual steps of the viral life cycle, we ruled out a role for PCBP1 in viral entry, translation, genome stability and viral RNA replication. Further analysis of the assembly step revealed that, similarly to its paralog hnRNP K, endogenous PCBP1 limits HCV virion assembly and release.

MATERIALS AND METHODS

Cell culture

Huh-7.5 human hepatoma cells were obtained from Charlie Rice (Rockefeller University) and maintained in complete media: Dulbecco's Modified Eagle Media (DMEM) supplemented with inactivated 10% fetal bovine serum (FBS), 2 mM L-glutamine, and 1X MEM non-essential amino acids. Human embryonic kidney (293T) cells were kindly provided by Martin J. Richer (McGill University, Montreal, QC, Canada) and were maintained in DMEM supplemented with 10% FBS. All cell lines were maintained at 37°C/5% CO_2 and were routinely screened for mycoplasma contamination.

92 **Plasmids and viral RNAs**

93 The pJFH-1$_T$ plasmid, encoding a cell culture-adapted Japanese Fulminant Hepatitis (JFH-1;
94 HCV genotype 2a) with three adaptive mutations that increase viral titers in cell culture, was a
95 gift from Rodney Russell (Memorial University of Newfoundland) (18). Plasmids pJ6/JFH1 FL
96 RLuc WT ("RLuc-wt") and pJ6/JFH-1 FL RLuc GNN ("RLuc-GNN") bear full-length viral
97 sequence derived from the J6 (structural genes) and JFH-1 (NS genes) isolates of HCV, with a
98 *Renilla* luciferase (RLuc) reporter (5). The pJ6/JFH-1 mono RLuc-NS2 plasmid ("Δcore-p7") – a
99 truncated version of the *Renilla* reporter virus with a deletion of the structural genes through p7 –
100 was a gift from Joyce Wilson (University of Saskatchewan) (19). The pJ6/JFH-1 FL RLuc-
101 NS5A-GFP ("NS5A-GFP") was created via overlapping PCR and subcloned using the *AvrII* and
102 *XbaI* restriction sites, as previously described (20).

103 To make full-length uncapped viral RNAs, all plasmid templates were linearized and *in*
104 *vitro* transcribed as previously described (21). The firefly luciferase (FLuc) mRNA was transcribed
105 from the Luciferase T7 Control DNA plasmid (Promega) linearized using *XmnI* and *in vitro*
106 transcribed using the mMessage mMachine T7 Kit (Life Technologies) according to the
107 manufacturer's instructions.

108

109 **Generation of infectious HCV stocks**

110 To generate viral stocks, 30 µg of *in vitro* transcribed JFH-1$_T$ RNA was transfected into Huh-7.5
111 cells using the DMRIE-C reagent (Life Technologies) according to the manufacturer's
112 instructions. Four days post-transfection, infectious cell supernatants were passed through a 0.45
113 µm filter and infectious viral titers were determined by focus-forming unit assay (18). Infectious

114 virus was amplified for two passages through Huh-7.5 cells at a MOI of 0.1. Viral stocks were
115 aliquoted and stored at -80°C until use.
116
117 **Focus-forming unit (FFU) assays**
118 One day prior to infection, 8-well chamber slides (Lab-Tek) were seeded with 4 x 10^5 Huh-7.5
119 cells/well. Infections were performed with 10-fold serial dilutions of viral samples in 100 µL for
120 4 h, after which the supernatant was replaced with fresh media. Three days post-infection, slides
121 were fixed in 100% acetone and stained with anti-HCV core antibody (1:100, clone B2,
122 Anogen), and subsequently with the AlexaFluor-488-conjugated anti-mouse antibody (1:200,
123 ThermoFisher Scientific) for immunofluorescence analysis. Viral titers are expressed as the
124 number of focus-forming units (FFU) per mL.
125 Extracellular virus titers were determined directly from cell supernatants, while
126 intracellular virus titers were determined after cell pellets were subjected to lysis via four freeze-
127 thaw cycles, removal of cellular debris via centrifugation, and recovery of virus-containing
128 supernatants.
129
130 **MicroRNAs and siRNA sequences**
131 siGL3 (siCTRL): 5'-CUUACGCUGAGUACUUCGAUU-3', siGL3* : 5'-
132 UCGAAGUACUCAGCGUAAGUU-3', miR122$_{p2\text{-}8}$ (siCTRL for luciferase experiments): 5'-
133 UAAUCACAGACAAUGGUGUUUGU-3', miR122$_{p2\text{-}8}$*: 5'-
134 AAACGCCAUUAUCUGUGAGGAUA-3' (22), siPCBP1: 5'-
135 CUGUGUAAUUUCUGGUCAGUU-3', siPCBP1*: 5'-CUGACCAGAAAUUACACAGUU-3'
136 (17) were all synthesized by Integrated DNA Technologies.

All microRNA and siRNA duplexes were diluted to a final concentration of 20 µM in RNA annealing buffer (150 mM HEPES pH 7.4, 500 mM potassium acetate, 10 mM magnesium acetate), and annealed at 37°C for 1 h and stored at -20°C. For all knockdown experiments, 50 nM siRNA transfections were conducted 2 days prior to infection or electroporation of viral RNAs. Transfections were conducted using the Lipofectamine RNAiMAX (Invitrogen) according to the manufacturer's instructions with the modification that 20 µL of reagent were used to transfect a 10-cm dish of cells.

HCV and VSV pseudoparticles (HCVpp and VSVpp)

HCVpp consisting of a FLuc reporter lentiviral vector pseudotyped with the HCV E1 and E2 glycoprotein (from the H77, a genotype 1a strain) were a kind gift from John Law (University of Alberta) (23). To generate lentiviral vectors pseudotyped with the VSV-G glycoprotein (VSVpp), a 90% confluent 10-cm dish of 293T cells were transfected with 10 µg pPRIME-FLuc, 5 µg psPAX.2, and 2.5 µg pVSV-G plasmid with 10 µL Lipofectamine 2000 (Invitrogen) diluted in 4 mL Opti-MEM. Media was changed 4, 20, and 28 h post-transfection. At 48 h post-transfection, the cell culture media was passed through a 0.45 µm filter and stored at -80°C.

To assay for cell entry, HCVpp and VSVpp were diluted 1/3 in dilution media (1X DMEM, 3% FBS, 100 IU penicillin and 100 µg/mL streptomycin) with 20 mM HEPES and 4 µg/µL polybrene, and then introduced to Huh-7.5 cells by spinoculation at 1,200 rpm for 1 h at room temperature. The cells were left to recover at 37°C for at least 5 h before the pseudoparticle-containing media was changed for fresh complete Huh-7.5 media. In parallel, cells seeded in a 6-well plate were transfected with 1 µg of pPRIME-FLuc plasmid using Lipofectamine 2000 (Invitrogen) according to the manufacturer's instructions. Three days post-

spinoculation and transfection, cells were lysed in passive lysis buffer (Promega) and FLuc activity was assayed using the Dual Reporter Luciferase kit (Promega).

Electroporations

For each electroporation, 400 µL of resuspended cells (1.5 x 10^7 cell/mL) were mixed with 2 µg of FLuc mRNA and 5 µg of replicating (WT, Δcore-p7 or NS5A-GFP J6/JFH-1 RNA) or 10 µg GNN J6/JFH-1 RNA, and electroporated in 4-mm cuvettes at 270 V, 950 µF, and infinite resistance, optimized for the Bio-Rad GenePulser XCell (Bio-Rad). Electroporated cells were resuspended in complete Huh-7.5 media and transferred to 6-well plates for luciferase assays and protein analysis.

Inhibition of RNA replication by 2´CMA

Two days post-siRNA transfection, Huh-7.5 cells were infected with JFH-1_T at a MOI of 0.05. Four to five hours post-infection, each plate of infected cells was split into 6-well plates. Three days post-infection, the media on these cells was changed for complete Huh-7.5 media with 5 µM 2´CMA (2´C-methyladenosine, Carbosynth), an HCV NS5B polymerase inhibitor, or DMSO control (24). Total RNA and intracellular virus samples were collected at 0, 6 and 12 h post-treatment, while cell culture supernatants were collected 6 and 12 h post-treatment. Protein samples were collected from untreated plates to assess PCBP1 knockdown efficiency by Western blot.

Western blot analysis

To collect total intracellular protein samples, cells were lysed in RIPA buffer (150 mM sodium chloride, 1% NP-40, 0.5% sodium deoxycholate, 0.1% SDS, 50 mM Tris pH 8.0, Complete Protease Inhibitor Cocktail (Roche)) and frozen at -80°C. Cellular debris was pelleted by centrifugation at 16,000 x g for 30 min at 4°C, and the supernatant was quantified by BCA Protein Assay (ThermoScientific). Ten micrograms of sample were loaded onto 10-12% SDS-PAGE gels. Samples were transferred onto Immobilon-P PVDF membranes (Millipore), blocked in 5% milk, and incubated overnight with primary antibodies diluted in 5% BSA: rabbit anti-PCBP1 (clone EPR11055, Abcam ab168378, 1:10,000); rabbit anti-actin (A2066, Sigma, 1:20,000); mouse anti-HCV core (clone B2, Anogen MO-I40015B, diluted 1:7,500); mouse anti-JFH-1 NS5A (clone 7B5, BioFront Technologies, 1:10,000). Blots were incubated for 1 hour with HRP-conjugated secondary antibodies diluted in 5% skim milk: anti-mouse (HAF007, R&D Systems, 1:25,000); anti-rabbit (111-035-144, Jackson ImmunoResearch Laboratories, 1:50,000) and visualized using enhanced chemiluminescence (ECL Prime Western Blotting Detection Reagent, Fisher Scientific).

RNA isolation and Northern blot analysis

Total RNA was harvested using TRIzol Reagent (ThermoFisher Scientific) according to the manufacturer's instructions. Ten micrograms of total RNA were separated on a 1% agarose gel containing 1X 3-(N-morpholino)propanesulfonic acid (MOPS) buffer and 2.2 M formaldehyde and transferred to a Zeta-probe membrane (Bio-Rad) by capillary transfer in 20X SSC buffer (3 M NaCl, 0.3 M sodium citrate). Membranes were hybridized in ExpressHyb Hybridization Buffer (ClonTech) to random-primed ^{32}P-labeled DNA probes (RadPrime DNA labelling

system, Life Technologies) complementary to HCV (nt 84-374) and γ-actin (nt 685-1171). Autoradiograph band densities were quantified using Fiji (25).

RT-qPCR analysis

The iTaq Universal Probes One-Step kit (Bio-Rad) was used to perform duplex assays probing for the HCV genome (NS5B-FW primer: 5'-AGACACTCCCCTATCAATTCATGGC-3'; NS5B-RV primer: 5'-GCGTCAAGCCCGTGTAACC-3'; NS5B-FAM probe: 5'-ATGGGTTCGCATGGTCCTAATGACACAC-3') and the GAPDH loading control (PrimePCR Probe assay with HEX probe, Bio-Rad). Each 20 µL reaction contained 500 ng of total RNA, 1.5 µL of the HCV primers and probe, and 0.5 µL of the GAPDH primers and probe. RT-PCR reactions were conducted in a CFX96 Touch Deep Well Real-Time PCR system (Bio-Rad). Genome copies were calculated using a standard curve and fold-differences in gene expression were calculated using the $2^{-\Delta\Delta Ct}$ method (26).

Luciferase assays

For translation and replication assays, cells were washed in PBS and harvested in 100 µL of 1X passive lysis buffer (Promega). The Dual-Luciferase Assay Reporter Kit (Promega) was used to measure both *Renilla* and firefly luciferase activity according to the manufacturer's instructions with the modification that 25 µL of reagent were used with 10 µL of sample. All samples were measured in triplicate.

225 **Data analysis**

226 Statistical analyses were performed using GraphPad Prism v9 (GraphPad, USA). Statistical
227 significance was determined by paired t-test to compare results obtained from multiple
228 experiments, and by two-way ANOVA with Geisser-Greenhouse and Bonferroni corrections
229 when more than two comparisons were applied at once. To calculate half-lives, a one-step decay
230 curve using the least-squares regression was used, and error was reported as the asymmetrical
231 (profile likelihood) 95% confidence interval of the half-life. To calculate virus accumulation and
232 virus secretion rates, a simple linear regression was performed using the least squares regression
233 method. The slope and standard error calculated for each regression represents the rate of virus
234 accumulation or secretion.

235

236 **RESULTS**

237 **PCBP1 plays a role in the HCV life cycle**

238 The PCBP1 protein was previously reported to directly interact with the 5′ UTR of the HCV
239 genome, and in an siRNA screen PCBP1 knockdown resulted in a reduction in HCV RNA
240 accumulation (11, 17). Thus, we sought to further characterize the role of PCBP1 in the HCV life
241 cycle. We began by assessing how PCBP1 knockdown affected the accumulation of cell culture-
242 derived HCV (HCVcc), using the cell-culture adapted JFH-1_T strain. Compared to the parental
243 JFH-1 strain, JFH-1_T has three adaptive mutations in the E2, p7 and NS2 coding-region, which
244 enable it to produce higher viral titers in cell culture (18). We found that knockdown of
245 endogenous PCBP1 resulted in an approximately 2.2-fold decrease in viral protein and RNA
246 accumulation in Huh-7.5 cells (**Figure 1A-C and Supplementary Figure 1**). Interestingly,
247 when we quantified intracellular and extracellular virions, we found that while intracellular titers

were not significantly different between the PCBP1 knockdown and control conditions, extracellular titers were elevated, with an average increase of approximately 3.90-fold in the PCBP1 knockdown condition (**Figure D-E**). Thus, in line with previous findings, we found that PCBP1 knockdown decreased viral protein expression and intracellular viral RNA accumulation. Yet, despite this overall decrease, we observed an increase in extracellular (secreted) virus titers. These results imply that endogenous PCBP1 indeed plays a role in the HCV life cycle, although the precise step(s) influenced by PCBP1 remain unclear.

PCBP1 knockdown has no impact on HCV entry

Firstly, we explored whether PCBP1 knockdown had any effect on virus entry. To this end, we made use of the HCV pseudoparticle (HCVpp) system, which consists of lentiviral vectors with a firefly luciferase reporter gene pseudotyped with the HCV E1 and E2 glycoproteins (23). HCVpp enter cells by clathrin-mediated endocytosis after engaging with HCV-specific entry receptors; thus, to account for any changes in clathrin-mediated endocytosis, we used a vesicular stomatitis virus (VSV) pseudoparticle system (VSVpp) as a control. In addition, to verify that PCBP1 knockdown did not affect luciferase reporter gene expression, we assessed firefly luciferase expression from cells directly transfected with a FLuc reporter plasmid. In all cases, we found that depleting endogenous PCBP1 had no impact on luciferase activity (**Figure 2**). This suggests that PCBP1 knockdown does not affect FLuc reporter expression, clathrin-mediated endocytosis, or the HCV entry process.

PCBP1 knockdown has no impact of HCV translation or genome stability

PCBP1 was previously reported to bind the HCV 5′ UTR, which contains the viral IRES that drives translation of the viral polyprotein in the absence of most canonical translation initiation factors (2, 3, 11, 27). Furthermore, PCBP1 has been reported to contribute to the IRES-mediated translation of some cellular mRNAs such as Bag-1 and *c-myc* (28-30). Thus, it was plausible that PCBP1's interactions with the viral 5′ UTR could affect viral protein expression by altering IRES-mediated translation. To assess PCBP1's impact on HCV translation, we used full-length J6/JFH-1 RLuc reporter RNAs containing an inactivating mutation in the NS5B polymerase gene (GNN). The RLuc activity thus served as a direct measure of HCV IRES-mediated translation, and over time, this signal also served as a proxy measure for viral RNA stability. We found that the siPCBP1 and siCTRL conditions had similar RLuc activity at all timepoints (**Figure 3**). Moreover, the luciferase signal half-lives were nearly identical, with 2.68 h (95% CI 1.64 – 4.64) for the siPCBP1 condition and 2.71 h (95% CI 1.43 – 5.50) for the siCTRL condition. Thus, PCBP1 knockdown does not appear to affect either viral IRES-mediated translation or genome stability.

PCBP1 knockdown does not affect viral RNA replication

PCBP1 has been reported to promote viral RNA replication by binding to the 5′ UTR of several RNA viruses (31, 32). Thus, to specifically assess whether PCBP1 knockdown has an effect on HCV RNA replication, we assessed RLuc expression of replication-competent but assembly-deficient reporter RNAs (**Figure 4**). This includes the full-length WT J6/JFH-1 RLuc RNA, a subgenomic J6/JFH-1 replicon RNA containing a deletion of the structural protein genes (Δcore-

p7), and a full-length J6/JFH-1 genome with a GFP insertion in the NS5A gene (NS5A-GFP), the latter previously shown to impair virion assembly without impairing viral RNA replication (7, 20). In all cases, we did not observe any significant differences in viral RNA accumulation between the siPCBP1 and siCTRL conditions (**Figure 4A-C**). This is seemingly in contrast to our findings using the JFH-1_T system, where PCBP1 depletion decreased viral RNA accumulation (**Figure 1B-C and Supplementary Figure 1**). However, it is notable that all of the viral RNAs used in **Figure 4** are defective in viral packaging, including the full-length WT J6/JFH-1 RLuc RNA (**Figure 4A**), likely due to the large RLuc reporter gene insertion (**Supplementary Figure 2**). Thus, taken together, our data suggests that PCBP1 has no effect on the viral RNA replication step of the HCV life cycle.

PCBP1 knockdown limits virus egress

Finally, since knockdown of PCBP1 did not seem to have a significant impact on HCV entry, translation, genome stability or viral RNA replication, we reasoned that PCBP1 was likely to be exerting an effect on virion assembly and/or secretion. We had previously established that PCBP1 knockdown did not have a significant effect on intracellular viral titers yet resulted in an overall increase in extracellular (secreted) virions (**Figure 1D-E**). Thus, to further investigate whether PCBP1 plays a role in viral packaging and/or egress, we used a nucleoside analog, 2′C-methyladenosine (2′CMA), to block viral RNA synthesis by the HCV NS5B RNA-dependent RNA polymerase and monitored viral titers over time (24). Similar to related studies using Zika virus, we reasoned that blocking viral RNA synthesis could allow us to assess viral packaging and egress in the absence of genomic RNA production (33).

To this end, we infected cells with JFH-1_T and, three days post-infection, we replaced the culture media with media containing 5 μM 2′CMA (or DMSO, as a control) and collected total RNA, intracellular virions and extracellular virions over the next 12 h (**Figure 5A**). In agreement with our previous findings, we observed an overall reduction in JFH-1_T viral RNA accumulation by day 3 post-infection in the siPCBP1 condition (0 h timepoint, **Figure 5B**). In addition, the 2′CMA treatment efficiently blocked viral RNA accumulation, which continued to increase under the control (DMSO) condition (6-12 h timepoints, **Figure 5B**). Additionally, we observed similar initial intracellular titers as well as similar 2′CMA-induced decreases in intracellular titers under both the siPCBP1 and siCTRL conditions (**Figure 5C and D**). In contrast, we observed a continued rise in extracellular titers as packaged viruses continued to egress out of the cell, with the PCBP1 knockdown resulting in a >3-fold greater virus secretion rate than the siCTRL condition during 2′CMA treatment (**Figure 5E and F**). Notably, since inhibiting viral RNA synthesis equalized the intracellular virus accumulation rates yet failed to equalize the virus secretion rates, these results suggest that PCBP1 modulates the virion assembly and egress steps of the HCV life cycle.

DISCUSSION

Herein, we investigated the role of PCBP1 in the HCV life cycle. We found that PCBP1 knockdown did not directly affect virus entry, translation, genome stability or viral RNA replication; but resulted in an increase in infectious particle secretion. Furthermore, since PCBP1 knockdown does not alter intracellular infectious particle accumulation yet reduces total intracellular viral RNA, our results suggest that PCBP1 knockdown promotes virion assembly and egress.

Previous studies had found that PCBP1 interacts with the HCV 5′ UTR *in vitro* (11, 16). Notably, the full 5′ UTR appeared to be critical for PCBP1 binding, as truncated fragments of the 5′ UTR were unable to bind to PCBP1 (11, 16). Somewhat more recently, PCBP1 was one of many host factors evaluated in a siRNA screen targeting cellular proteins predicted to interact with HCV (17). This screen revealed that PCBP1 knockdown decreased viral RNA accumulation approximately 2.3-fold, a result consistent with our observation that PCBP1 knockdown decreased JFH-1_T viral RNA accumulation by approximately 2.2-fold (**Figure 1D**) (17). However, our systematic evaluation of the effect of PCBP1 knockdown on viral translation and viral RNA replication revealed that PCBP1 does not modulate either of these steps in the viral life cycle. Moreover, we did not observe any significant effects on viral entry or genome stability.

Initially, we were quite puzzled to find that PCBP1 did not affect viral RNA accumulation of a full-length WT J6/JFH-1 RLuc RNA; however, this RNA generates far fewer infectious viral particles than the JFH-1_T strain we used for our infection experiments, likely due to the increased genome size due to the RLuc insertion resulting in reduced packaging efficiency (**Supplementary Figure S2**) (14). The fact that PCBP1 knockdown failed to have a significant impact on the luciferase reporter RNA is therefore consistent with a model whereby PCBP1 primarily acts at the level of virion assembly and egress (**Figure 6**). As such, knockdown of PCBP1 results in an overall decrease in the translating/replicating pool of viral RNAs and a concomitant increase in extracellular (secreted) virions. Since intracellular viral titers remained similar in PCBP1 knockdown and control conditions, a greater proportion of the intracellular viral RNA must represent viral RNA packaged into virions, implying that endogenous PCBP1 normally limits virion assembly. This model is further supported by our finding that 2′CMA

equalized the rate of intracellular virus accumulation yet resulted in a virus secretion rate >3-fold greater during PCBP1 knockdown, suggesting that endogenous PCBP1 limits virion egress. Moreover, this model is consistent with the observed decreases in viral protein expression and negative-strand replicative intermediate accumulation (**Figure 1B and Supplementary Figure 1**), since increasing viral genome packaging into new virions would sequester the RNA from the translation and RNA replication machinery. Thus, endogenous PCBP1 normally limits viral assembly and egress, and PCBP1 knockdown therefore indirectly impairs viral protein synthesis and viral RNA replication by liberating the RNA for virion assembly and egress.

Notably, PCBP1 has been previously implicated in turnover of MAVS, a signal transduction protein directly downstream of RIG-I, which is known to limit HCV infection (34). However, all of our conclusions were drawn from experiments conducted in the Huh-7.5 cell line, which has well-documented defects in the RIG-I antiviral signalling pathway, and our own brief explorations of interferon induction and MAVS turnover did not reveal any significant differences between PCBP1 knockdown and control conditions (data not shown) (35). Moreover, the HCV NS3-4A protease also inactivates MAVS during infection to reduce antiviral signaling and recognition of the viral RNA (36, 37). However, as hepatocytes typically express RIG-I and MAVS, we cannot rule out the possibility that PCBP1 may modulate this pathway during infection *in vivo*.

Finally, PCBP1's closely related paralogs, hnRNP K and PCBP2, have been more extensively studied during HCV infection. While the hnRNP K protein was shown to restrict infectious virion production, the PCBP2 protein has been suggested to modulate viral translation and RNA replication (14, 15). Since the PCBP1 amino acid identity is far more similar to PCBP2 (~80% identity) than hnRNP K (~24% identity), we were initially surprised that our findings for

382 PCBP1 in HCV infection closely matched those reported for hnRNP K. Yet, while PCBP1 and
383 PCBP2 have been shown to perform similar functions, they have also been reported to play
384 distinct roles during poliovirus, VSV, and human immunodeficiency virus infection (31, 38, 39).
385 In addition to the similarities we observed with PCBP1 and those previously reported with
386 hnRNP K during HCV infection, our results and conclusions also echo those reported for the
387 IGF2BP2/YBX-1 complex, METTL3/METTL14 *N*6-methyladenosine (m^6A) writers, and the
388 YTHDF m^6A-binding proteins (14, 40, 41). These have all been reported to inhibit HCV
389 infectious particle production, with no effect on viral translation or RNA replication – with the
390 exception of the IGF2BP2/YBX-1 complex, which plays an additional role in facilitating viral
391 RNA replication (40). It is currently unclear if PCBP1, hnRNP K, the YBX-1 complex or m^6A
392 modifications of the HCV genome inhibit virion assembly as components of a common pathway,
393 or through distinct and/or additive mechanisms. Interestingly, high-throughput affinity capture
394 and proximity ligation studies have found that PCBP1 interacts with hnRNP K, IGF2BP2, YBX-
395 1, METTL3 and METTL14; although this has been demonstrated only in non-hepatic cell lines
396 to date (42-44). Should these interactions be conserved during HCV infection, it seems plausible
397 that PCBP1 could participate in these virion assembly inhibition pathways – or, conversely, that
398 it may have an inhibitory role to promote one pathway over another. Future investigations will
399 reveal whether these proteins function in an overlapping or a distinct manner; and are likely to
400 improve our understanding of HCV virion assembly and how this process is regulated by cellular
401 RNA binding proteins.

402 Taken together, our results support a model where endogenous PCBP1 limits HCV
403 infectious particle production. By preventing virion assembly and egress, PCBP1 indirectly
404 enhances viral RNA accumulation. The model presented herein helps to inform understanding of

405 how cellular RNA-binding proteins modulate HCV genomic RNA utilization during the viral life
406 cycle, specifically as it pertains to virion assembly. While the precise molecular mechanism
407 employed by PCBP1 to inhibit HCV assembly and egress remains to be characterized, similar
408 phenotypes reported for hnRNP K, IGF2BP2/YBX-1 and m^6A modifications of the HCV
409 genome offer promising leads for future investigations.

ACKNOWLEDGEMENTS

We would like to acknowledge Charlie Rice (Rockefeller University) for kindly providing the Huh-7.5 cells, pJ6/JFH FL RLuc WT and GNN plasmids; Rodney Russell (Memorial University) for providing JFH-1_T; Mamata Panigrahi and Joyce Wilson (University of Saskatchewan) for the pJ6/JFH mono RLuc NS2 plasmid; Martin J Richer (McGill University) for the 293T cells; and John Law (University of Alberta) for supplying the HCVpp used herein. We are also grateful to Nathan Taylor, Julie Magnus and Carolina Camargo (McGill University) for technical support.

FUNDING INFORMATION

This research was supported by the Canadian Institutes for Health Research (CIHR) [MOP-136915 and PJT-169214]. S.E.C. was supported by the Canadian Network on Hepatitis C (CanHepC) training program, as well as a Vanier Canada Graduate Scholarship. In addition, this research was undertaken, in part, thanks to the Canada Research Chairs program (S.M.S.).

AUTHOR CONTRIBUTIONS

S.E.C. and S.M.S. designed the study; S.E.C. performed the experiments and analyzed the data, and S.E.C and S.M.S. wrote and edited the manuscript.

REFERENCES

1. **Simmonds P**, **Becher P**, **Bukh J**, **Gould EA**, **Meyers G**, **Monath T**, **Muerhoff S**, **Pletnev A**, **Rico-Hesse R**, **Smith DB**, **Stapleton JT**, **ICTV Report Consortium**. 2017. ICTV Virus Taxonomy Profile: Flaviviridae. J Gen Virol **98**:2–3.

2. **Tsukiyama-Kohara K**, **Iizuka N**, **Kohara M**, **Nomoto A**. 1992. Internal ribosome entry site within hepatitis C virus RNA. Journal of Virology **66**:1476–1483.

3. **Lancaster AM**, **Jan E**, **Sarnow P**. 2006. Initiation factor-independent translation mediated by the hepatitis C virus internal ribosome entry site. RNA **12**:894–902.

4. **Lohmann V**, **Korner F**, **Koch J**, **Herian U**, **Theilmann L**, **Bartenschlager R**. 1999. Replication of subgenomic hepatitis C virus RNAs in a hepatoma cell line. Science **285**:110–113.

5. **Jones CT**, **Murray CL**, **Eastman DK**, **Tassello J**, **Rice CM**. 2007. Hepatitis C virus p7 and NS2 proteins are essential for production of infectious virus. Journal of Virology **81**:8374–8383.

6. **Jones DM**, **Atoom AM**, **Zhang X**, **Kottilil S**, **Russell RS**. 2011. A genetic interaction between the core and NS3 proteins of hepatitis C virus is essential for production of infectious virus. Journal of Virology **85**:12351–12361.

7. **Masaki T**, **Suzuki R**, **Murakami K**, **Aizaki H**, **Ishii K**, **Murayama A**, **Date T**, **Matsuura Y**, **Miyamura T**, **Wakita T**, **Suzuki T**. 2008. Interaction of hepatitis C virus nonstructural protein 5A with core protein is critical for the production of infectious virus particles. Journal of Virology **82**:7964–7976.

8. **Appel N**, **Zayas M**, **Miller S**, **Krijnse-Locker J**, **Schaller T**, **Friebe P**, **Kallis S**, **Engel U**, **Bartenschlager R**. 2008. Essential role of domain III of nonstructural protein 5A for hepatitis C virus infectious particle assembly. PLoS Pathog **4**:e1000035.

9. **Matunis MJ**, **Michael WM**, **Dreyfuss G**. 1992. Characterization and primary structure of the poly(C)-binding heterogeneous nuclear ribonucleoprotein complex K protein. Mol Cell Biol **12**:164–171.

10. **Du Z**, **Lee JK**, **Fenn S**, **Tjhen R**, **Stroud RM**, **James TL**. 2007. X-ray crystallographic and NMR studies of protein-protein and protein-nucleic acid interactions involving the KH domains from human poly(C)-binding protein-2. RNA **13**:1043–1051.

11. **Spångberg K**, **Schwartz S**. 1999. Poly(C)-binding protein interacts with the hepatitis C virus 5' untranslated region **80**:1371–1376.

12. **Flynn RA**, **Martin L**, **Spitale RC**, **Do BT**, **Sagan SM**, **Zarnegar B**, **Qu K**, **Khavari PA**, **Quake SR**, **Sarnow P**, **Chang HY**. 2015. Dissecting noncoding and pathogen RNA-protein interactomes. RNA **21**:135–143.

13. **Fan B**, **Lu K-Y**, **Reymond Sutandy FX**, **Chen Y-W**, **Konan K**, **Zhu H**, **Kao CC**, **Chen C-S**. 2014. A human proteome microarray identifies that the heterogeneous nuclear ribonucleoprotein K (hnRNP K) recognizes the 5' terminal sequence of the hepatitis C virus RNA. Mol Cell Proteomics **13**:84–92.

14. **Poenisch M**, **Metz P**, **Blankenburg H**, **Ruggieri A**, **Lee J-Y**, **Rupp D**, **Rebhan I**, **Diederich K**, **Kaderali L**, **Domingues FS**, **Albrecht M**, **Lohmann V**, **Erfle H**, **Bartenschlager R**. 2015. Identification of HNRNPK as Regulator of Hepatitis C Virus Particle Production. PLoS Pathog **11**:e1004573–21.

15. **Wang L**, **Jeng K-S**, **Lai MMC**. 2011. Poly(C)-binding protein 2 interacts with sequences required for viral replication in the hepatitis C virus (HCV) 5' untranslated region and directs HCV RNA replication through circularizing the viral genome. Journal of Virology **85**:7954–7964.

16. **Choi K**, **Kim JH**, **Li X**, **Paek KY**, **Ha SH**, **Ryu SH**, **Wimmer E**, **Jang SK**. 2004. Identification of cellular proteins enhancing activities of internal ribosomal entry sites by competition with oligodeoxynucleotides. Nucleic Acids Research **32**:1308–1317.

17. **Randall G**, **Panis M**, **Cooper JD**, **Tellinghuisen TL**, **Sukhodolets KE**, **Pfeffer S**, **Landthaler M**, **Landgraf P**, **Kan S**, **Lindenbach BD**, **Chien M**, **Weir DB**, **Russo JJ**, **Ju J**, **Brownstein MJ**, **Sheridan R**, **Sander C**, **Zavolan M**, **Tuschl T**, **Rice CM**. 2007. Cellular cofactors affecting hepatitis C virus infection and replication. PNAS **104**:12884–12889.

18. **Russell RS**, **Meunier J-C**, **Takikawa S**, **Faulk K**, **Engle RE**, **Bukh J**, **Purcell RH**, **Emerson SU**. 2008. Advantages of a single-cycle production assay to study cell culture-adaptive mutations of hepatitis C virus. Proc Natl Acad Sci USA **105**:4370–4375.

19. **Panigrahi M**, **Thibault PA**, **Wilson JA**. 2021. Chapter 7: miR-122 affects both the early and late stages of a Hepatitis C Virus infection, pp. 129–165. *In* miR-122-independent propagation of Hepatitis C Virus: Understanding the underlying mechanism through characterization of viral replication [dissertation]. Saskatoon: University of Saskatchewan; 2021.

20. **Moradpour D**, **Evans MJ**, **Gosert R**, **Yuan Z**, **Blum HE**, **Goff SP**, **Lindenbach BD**, **Rice CM**. 2004. Insertion of green fluorescent protein into nonstructural protein 5A allows direct visualization of functional hepatitis C virus replication complexes. Journal of Virology **78**:7400–7409.

21. **Amador-Cañizares Y**, **Bernier A**, **Wilson JA**, **Sagan SM**. 2018. miR-122 does not impact recognition of the HCV genome by innate sensors of RNA but rather protects the 5′ end from the cellular pyrophosphatases, DOM3Z and DUSP11. Nucleic Acids Research **46**:5139–5158.

22. **Machlin ES**, **Sagan SM**, **Sarnow P**. 2011. Masking the 5' terminal nucleotides of the hepatitis C virus genome by an unconventional microRNA-target RNA complex. PNAS **108**:3193–3198.

23. **Hsu M**, **Zhang J**, **Flint M**, **Logvinoff C**, **Cheng-Mayer C**, **Rice CM**, **McKeating JA**. 2003. Hepatitis C virus glycoproteins mediate pH-dependent cell entry of pseudotyped retroviral particles. PNAS **100**:7271–7276.

24. **Carroll SS**, **Tomassini JE**, **Bosserman M**, **Getty K**, **Stahlhut MW**, **Eldrup AB**, **Bhat B**, **Hall D**, **Simcoe AL**, **LaFemina R**, **Rutkowski CA**, **Wolanski B**, **Yang Z**, **Migliaccio G**, **De Francesco R**, **Kuo LC**, **MacCoss M**, **Olsen DB**. 2003. Inhibition of hepatitis C virus RNA replication by 2'-modified nucleoside analogs. Journal of Biological Chemistry **278**:11979–11984.

25. **Schindelin J**, **Arganda-Carreras I**, **Frise E**, **Kaynig V**, **Longair M**, **Pietzsch T**, **Preibisch S**, **Rueden C**, **Saalfeld S**, **Schmid B**, **Tinevez J-Y**, **White DJ**, **Hartenstein V**, **Eliceiri K**, **Tomancak P**, **Cardona A**. 2012. Fiji: an open-source platform for biological-image analysis. Nat Meth **9**:676–682.

26. **Livak KJ**, **Schmittgen TD**. 2001. Analysis of Relative Gene Expression Data Using Real-Time Quantitative PCR and the 2−ΔΔCT Method. Methods **25**:402–408.

27. **Wang C**, **Sarnow P**, **Siddiqui A**. 1993. Translation of Human Hepatitis C Virus RNA in Cultured Cells Is Mediated by an Internal Ribosome-Binding Mechanism. Journal of Virology **67**:3338–3344.

28. **Le Quesne JPC**, **Stoneley M**, **Fraser GA**, **Willis AE**. 2001. Derivation of a structural model for the c-myc IRES. Journal of Molecular Biology **310**:111–126.

29. **Pickering BM**, **Mitchell SA**, **Spriggs KA**, **Stoneley M**, **Willis AE**. 2004. Bag-1 internal ribosome entry segment activity is promoted by structural changes mediated by poly(rC) binding protein 1 and recruitment of polypyrimidine tract binding protein 1. Mol Cell Biol **24**:5595–5605.

30. **Evans JR**, **Mitchell SA**, **Spriggs KA**, **Ostrowski J**, **Bomsztyk K**, **Ostarek D**, **Willis AE**. 2003. Members of the poly (rC) binding protein family stimulate the activity of the c-myc internal ribosome entry segment in vitro and in vivo. Oncogene **22**:8012–8020.

31. **Walter BL**, **Parsley TB**, **Ehrenfeld E**, **Semler BL**. 2002. Distinct Poly(rC) Binding Protein KH Domain Determinants for Poliovirus Translation Initiation and Viral RNA Replication. Journal of Virology **76**:12008–12022.

32. **Luo Z**, **Dong X**, **Li Y**, **Zhang Q**, **Kim C**, **Song Y**, **Kang L**, **Liu Y**, **Wu K**, **Wu J**. 2014. PolyC-Binding Protein 1 Interacts with 5′-Untranslated Region of Enterovirus 71 RNA in Membrane-Associated Complex to Facilitate Viral Replication. PLoS ONE **9**:e87491–13.

33. **Taguwa S**, **Yeh M-T**, **Rainbolt TK**, **Nayak A**, **Shao H**, **Gestwicki JE**, **Andino R**, **Frydman J**. 2019. Zika Virus Dependence on Host Hsp70 Provides a Protective Strategy against Infection and Disease. CellReports **26**:906–920.e3.

34. **Zhou X**, **You F**, **Chen H**, **Jiang Z**. 2012. Poly(C)-binding protein 1 (PCBP1) mediates housekeeping degradation of mitochondrial antiviral signaling (MAVS). Cell Res **22**:717–727.

35. **Sumpter R**, **Loo Y-M**, **Foy E**, **Li K**, **Yoneyama M**, **Fujita T**, **Lemon SM**, **Gale M**. 2005. Regulating intracellular antiviral defense and permissiveness to hepatitis C virus RNA replication through a cellular RNA helicase, RIG-I. Journal of Virology **79**:2689–2699.

36. **Meylan E**, **Curran J**, **Hofmann K**, **Moradpour D**, **Binder M**, **Bartenschlager R**, **Tschopp J**. 2005. Cardif is an adaptor protein in the RIG-I antiviral pathway and is targeted by hepatitis C virus. Nature **437**:1167–1172.

37. **Bender S**, **Reuter A**, **Eberle F**, **Einhorn E**, **Binder M**, **Bartenschlager R**. 2015. Activation of Type I and III Interferon Response by Mitochondrial and Peroxisomal MAVS and Inhibition by Hepatitis C Virus. PLoS Pathog **11**:e1005264–30.

38. **Dinh PX**, **Beura LK**, **Panda D**, **Das A**, **Pattnaik AK**. 2011. Antagonistic effects of cellular poly(C) binding proteins on vesicular stomatitis virus gene expression. Journal of Virology, 3rd ed. **85**:9459–9471.

39. **Woolaway K**, **Asai K**, **Emili A**, **Cochrane A**. 2007. hnRNP E1 and E2 have distinct roles in modulating HIV-1 gene expression. Retrovirology **4**:28–18.

40. **Chatel-Chaix L**, **Germain M-A**, **Motorina A**, **Bonneil É**, **Thibault P**, **Baril M**, **Lamarre D**. 2013. A host YB-1 ribonucleoprotein complex is hijacked by hepatitis C virus for the control of NS3-dependent particle production. Journal of Virology **87**:11704–11720.

41. **Gokhale NS**, **McIntyre ABR**, **McFadden MJ**, **Roder AE**, **Kennedy EM**, **Gandara JA**, **Hopcraft SE**, **Quicke KM**, **Vazquez C**, **Willer J**, **Ilkayeva OR**, **Law BA**, **Holley CL**, **Garcia-Blanco MA**, **Evans MJ**, **Suthar MS**, **Bradrick SS**, **Mason CE**, **Horner SM**. 2016. N6-Methyladenosine in Flaviviridae Viral RNA Genomes Regulates Infection. Cell Host & Microbe **20**:654–665.

42. **Rosenbluh J**, **Mercer J**, **Shrestha Y**, **Oliver R**, **Tamayo P**, **Doench JG**, **Tirosh I**, **Piccioni F**, **Hartenian E**, **Horn H**, **Fagbami L**, **Root DE**, **Jaffe J**, **Lage K**, **Boehm JS**, **Hahn WC**. 2016. Genetic and Proteomic Interrogation of Lower Confidence Candidate Genes Reveals Signaling Networks in β-Catenin-Active Cancers. Cell Syst **3**:302–316.e4.

43. **Youn J-Y**, **Dunham WH**, **Hong SJ**, **Knight JDR**, **Bashkurov M**, **Chen GI**, **Bagci H**, **Rathod B**, **MacLeod G**, **Eng SWM**, **Angers S**, **Morris Q**, **Fabian M**, **Côté J-F**,

Gingras A-C. 2018. High-Density Proximity Mapping Reveals the Subcellular Organization of mRNA-Associated Granules and Bodies. Molecular Cell **69**:517–532.e11.

44. **Yue Y**, **Liu J**, **Cui X**, **Cao J**, **Luo G**, **Zhang Z**, **Cheng T**, **Gao M**, **Shu X**, **Ma H**, **Wang F**, **Wang X**, **Shen B**, **Wang Y**, **Feng X**, **He C**, **Liu J**. 2018. VIRMA mediates preferential m(6)A mRNA methylation in 3'UTR and near stop codon and associates with alternative polyadenylation. Cell Discov **4**:10.

576 **FIGURE LEGENDS**

577

578 **Figure 1. PCBP1 knockdown decreases viral protein expression and intracellular viral**
579 **RNA accumulation, but increases secreted virus titers. (A)** Schematic representation of the
580 HCVcc (JFH-1_T) infectious particles and genomic RNA used in infections. Huh-7.5 cells were
581 transfected with siPCBP1 or siCTRL at day -2, and at day 0 were infected with JFH-1_T (MOI =
582 0.05). Viral protein, Total RNA and intracellular and extracellular infectious virus were
583 harvested at day 3 post-infection. **(B)** Viral protein expression analysis by Western blot (ns
584 indicates non-specific band; and arrow indicates core and NS5A bands). **(C)** Viral RNA
585 accumulation analysis by Northern blot, and **(D)** quantification by densitometry. **(E)** Intracellular
586 and **(F)** extracellular (secreted) virus titers, quantified by FFU assay. All data are representative
587 of three independent replicates, and error bars represent the standard deviation of the mean. P-
588 values were calculated by paired t-test.

589

590 **Figure 2. PCBP1 knockdown has no effect on HCV entry.** Two days post-siRNA transfection,
591 cells were spinoculated with luciferase reporter pseudoparticles expressing the HCV E1/E2
592 glycoproteins (HCVpp) or the VSV-G glycoprotein (VSVpp). In parallel, cells were transfected
593 with a firefly luciferase expression plasmid. Samples were harvested 3 days post-
594 infection/transfection, and analyzed by luciferase assay. The HCVpp and pFLuc data is
595 representative of three independent replicates, while the VSVpp data is representative of two
596 independent replicates. Error bars represent the standard deviation of the mean.

597

598 **Figure 3. PCBP1 knockdown has no impact on HCV translation or genome stability. (A)**
599 Schematic representation of the J6/JFH-RLuc-GNN reporter RNA. **(B)** Huh-7.5 cells were
600 electroporated with J6/JFH-1-RLuc-GNN reporter RNAs and FLuc control mRNA, and
601 luciferase activity was monitored at several timepoints post-electroporation. All data are
602 representative of three independent replicates. Error bars on the y-axis represent the standard
603 deviation of the mean, while error bars on the x-axis indicate the range of sample harvest times
604 across replicates.
605
606 **Figure 4. PCBP1 knockdown does not affect viral RNA replication.** Two days post-siRNA
607 transfection, Huh-7.5 cells were electroporated with **(A)** full-length RLuc WT J6/JFH-1 RNA,
608 **(B)** Δcore-p7 J6/JFH-1 RLuc RNA, or **(C)** full-length NS5A-GFP J6/JFH-1 RLuc RNA. RLuc
609 values were normalized to the early timepoint (3h), to control for disparities in electroporation
610 efficiency between experiments. All data are representative of three independent replicates and
611 error bars represent the standard deviation of the mean.
612
613 **Figure 5. Viral particle production after 2´CMA treatment confirms that PCBP1**
614 **knockdown enhances virion secretion**. **(A)** Schematic representation of the experimental
615 approach for 2´CMA experiments: two days post-siRNA transfection, Huh-7.5 cells were
616 infected with JFH-1_T (MOI = 0.05). Three days post-infection, cells were treated with 2´CMA or
617 DMSO (control). Total RNA, intracellular and extracellular virus was collected at t = 0, 6 and 12
618 h post-treatment. **(B)** Quantitative RT-PCR analysis after 2´CMA treatment. **(C)** Intracellular
619 viral titers and **(D)** intracellular virus accumulation rate calculated by linear regression. **(E)**
620 Extracellular viral titers and **(F)** virus secretion rates calculated by linear regression. All data are

representative of three independent replicates and error bars in (B), (C) and (E) represent the standard deviation of the mean. Error bars in (D) and (F) represent the slopes of the linear regressions ± standard error. P-values were calculated by two-way ANOVA.

Figure 6. Model for PCBP1 effects on HCV assembly and egress. Under wild-type conditions, PCBP1 inhibits HCV assembly and egress, leaving the majority of intracellular viral RNAs to engage in protein translation and viral genome replication. However, during PCBP1 knockdown, a disinhibition of assembly and egress leads to an overall decrease in the translating/replicating pool of viral RNAs, and a concomitant increase in viral infectious particle production.

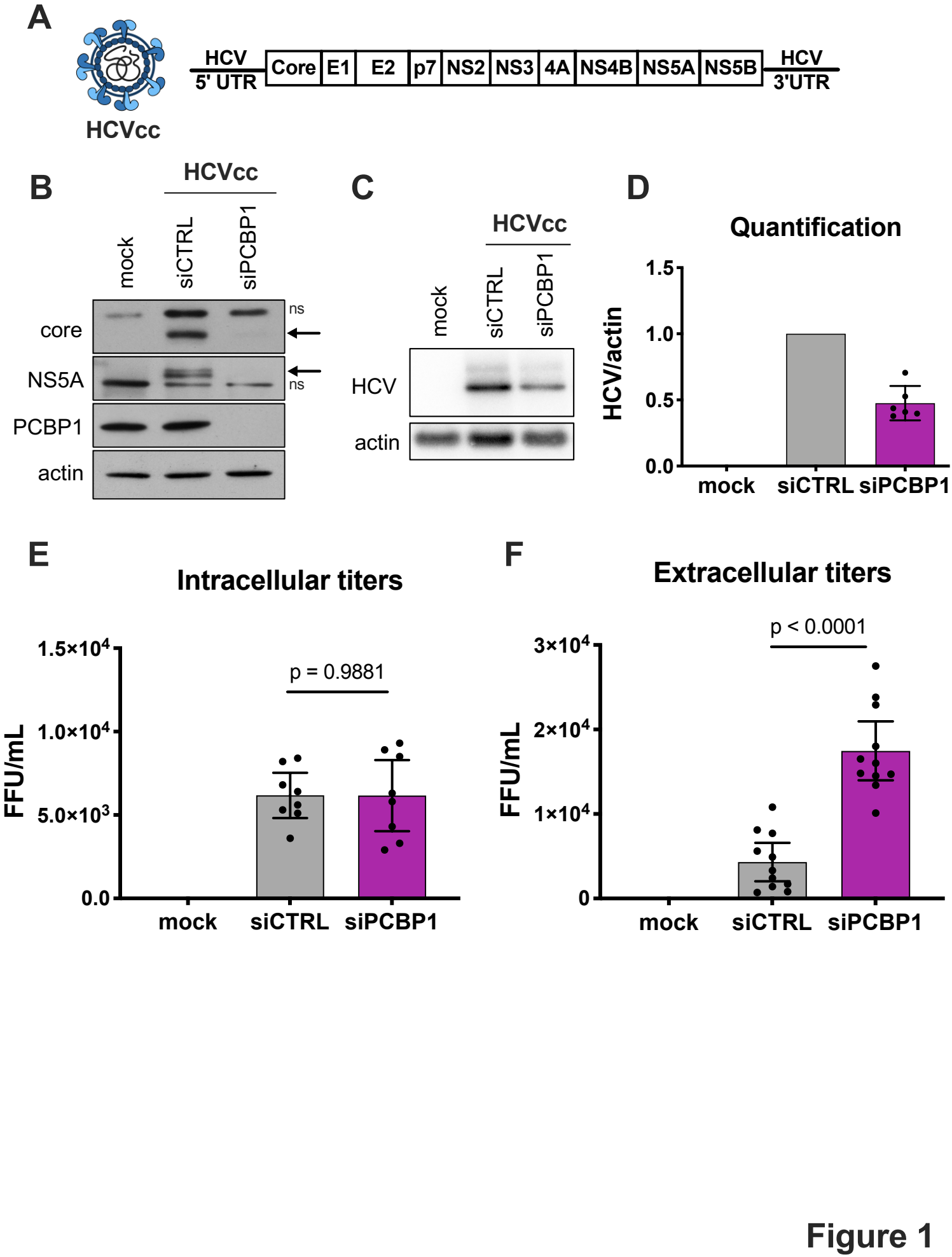
A
HCVcc
HCV 5' UTR
Core
E1
E2
p7
NS2
NS3
4A
NS4B
NS5A
NS5B
HCV 3'UTR
B
HCVcc
mock
siCTRL
siPCBP1
core
NS5A
PCBP1
actin
ns
ns
C
HCVcc
mock
siCTRL
siPCBP1
HCV
actin
D
Quantification
HCV/actin
1.5
1.0
0.5
0.0
mock
siCTRL
siPCBP1
E
Intracellular titers
FFU/mL
1.5×10^4
1.0×10^4
5.0×10^3
0.0
p = 0.9881
mock
siCTRL
siPCBP1
F
Extracellular titers
FFU/mL
3×10^4
2×10^4
1×10^4
0
p < 0.0001
mock
siCTRL
siPCBP1

Figure 1

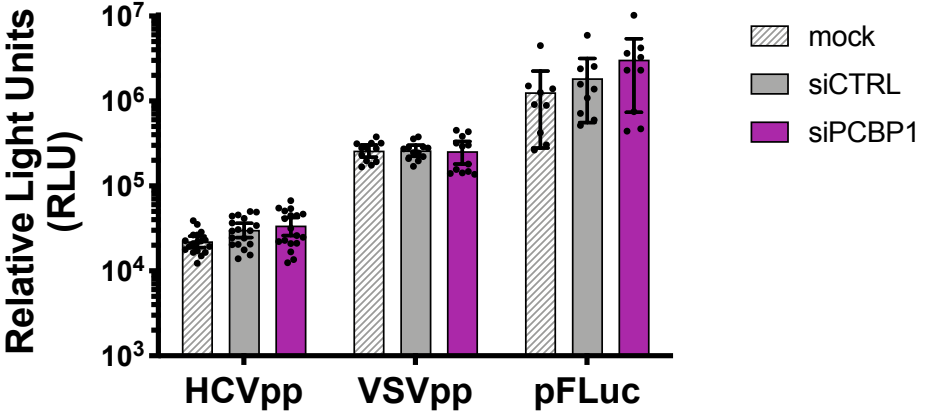
Relative Light Units (RLU)
10^7
10^6
10^5
10^4
10^3
HCVpp
VSVpp
pFLuc
mock
siCTRL
siPCBP1

Figure 2

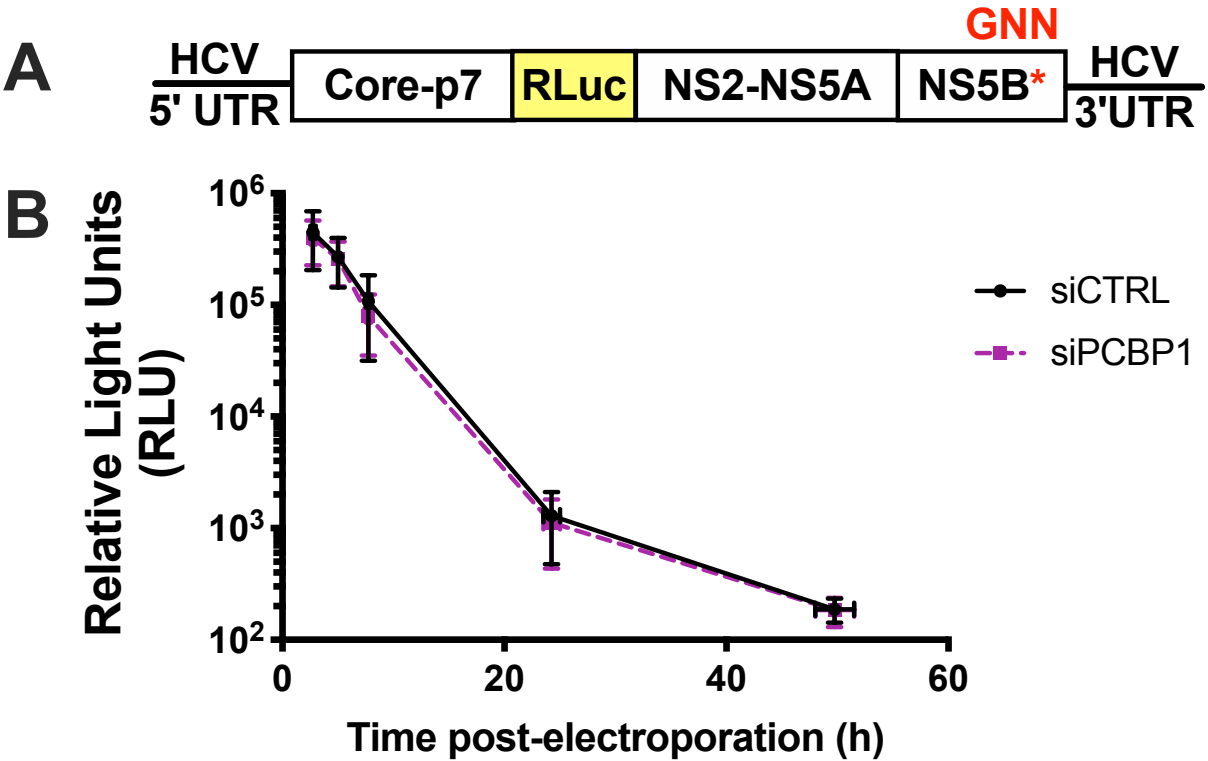
A
GNN
HCV
5' UTR
Core-p7
RLuc
NS2-NS5A
NS5B*
HCV
3'UTR
B
Relative Light Units
(RLU)
10^6
10^5
10^4
10^3
10^2
0
20
40
60
Time post-electroporation (h)
siCTRL
siPCBP1

Figure 3

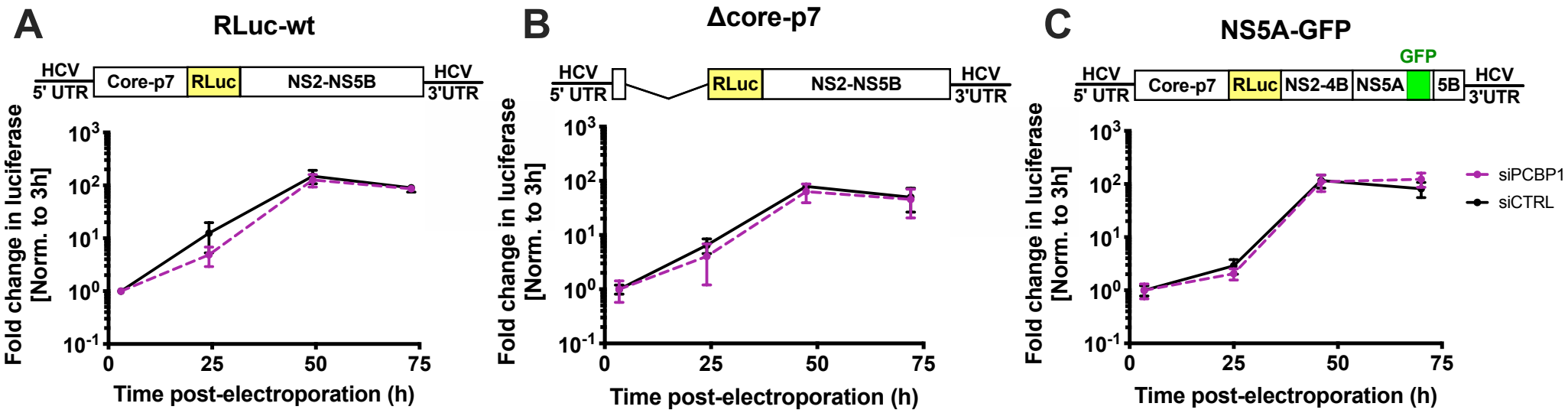
A
RLuc-wt
HCV 5' UTR
Core-p7
RLuc
NS2-NS5B
HCV 3'UTR
Fold change in luciferase [Norm. to 3h]
Time post-electroporation (h)
B
Δcore-p7
C
NS5A-GFP
GFP
NS2-4B
NS5A
5B
siPCBP1
siCTRL

Figure 4

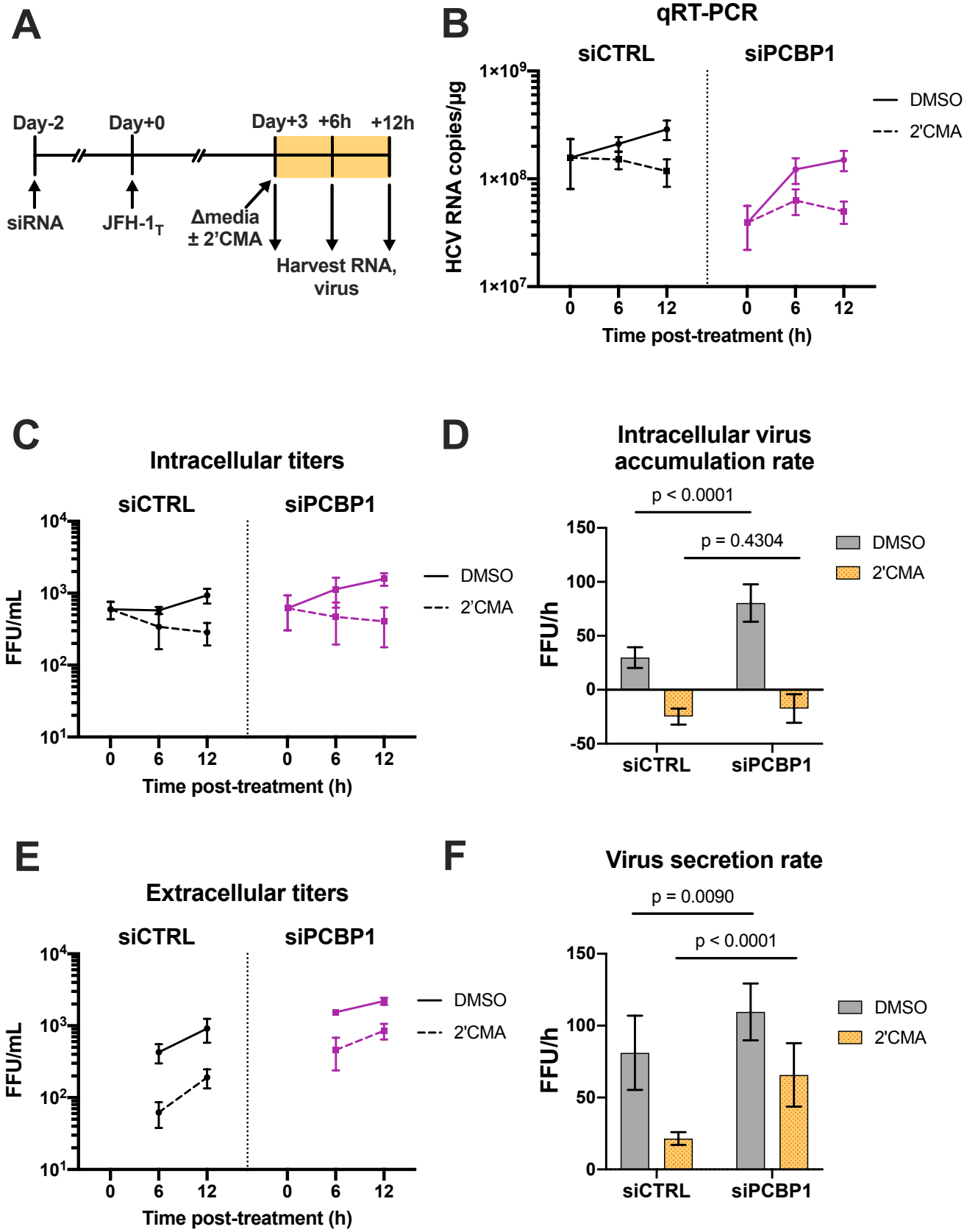
A
Day-2
Day+0
Day+3
+6h
+12h
siRNA
JFH-1T
Δmedia
± 2'CMA
Harvest RNA,
virus
B
qRT-PCR
siCTRL
siPCBP1
HCV RNA copies/µg
1×10^9
1×10^8
1×10^7
DMSO
2'CMA
0
6
12
Time post-treatment (h)
C
Intracellular titers
FFU/mL
10^4
10^3
10^2
10^1
D
Intracellular virus
accumulation rate
p < 0.0001
p = 0.4304
FFU/h
150
100
50
0
-50
E
Extracellular titers
F
Virus secretion rate
p = 0.0090
p < 0.0001

Figure 5

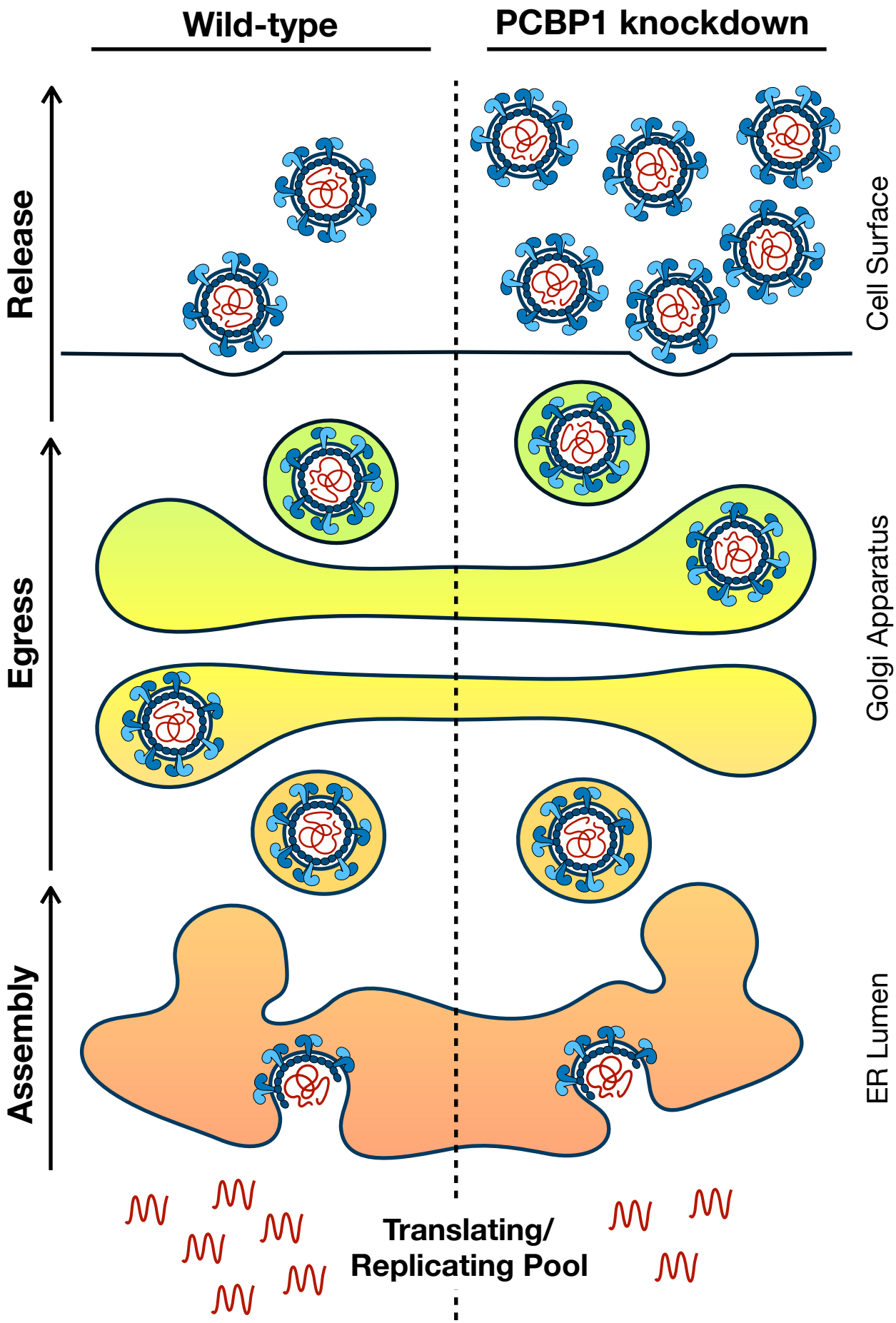

Figure 6

SUPPLEMENTARY MATERIAL

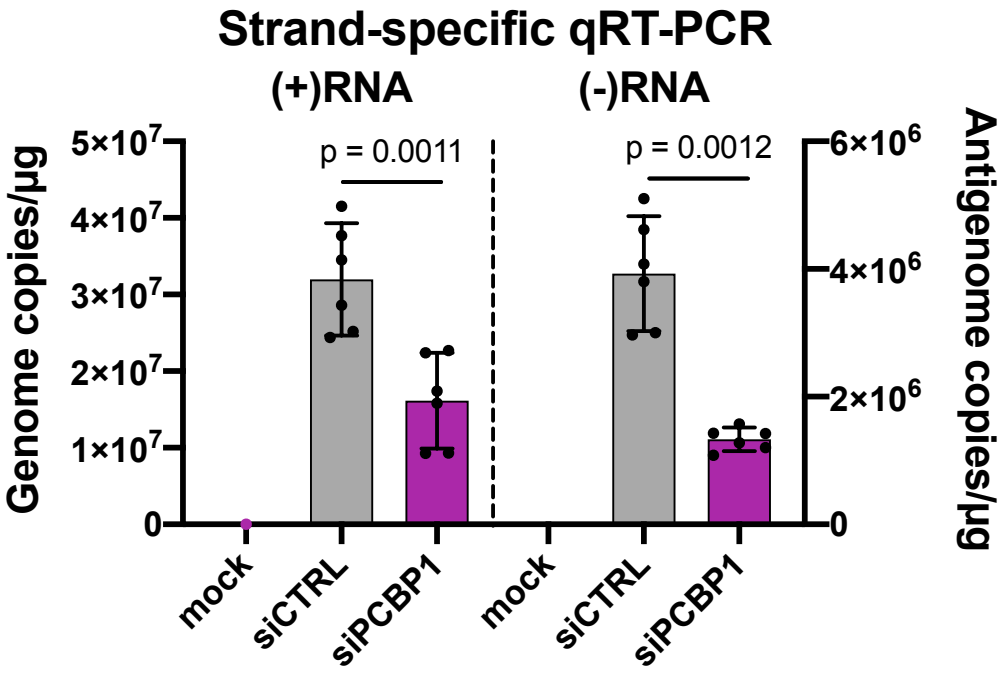

Supplementary Figure 1. PCBP1 knockdown decreases both positive-sense and negative-sense viral RNA accumulation. Two days post-siRNA transfection, Huh-7.5 cells were infected with JFH-1_T (MOI = 0.05). Total RNA was harvested 3 days post-infection and analysed by strand-specific RT-qPCR. All data is representative of three independent replicates and error bars represent the standard deviation. P-values were calculated by paired t-test.

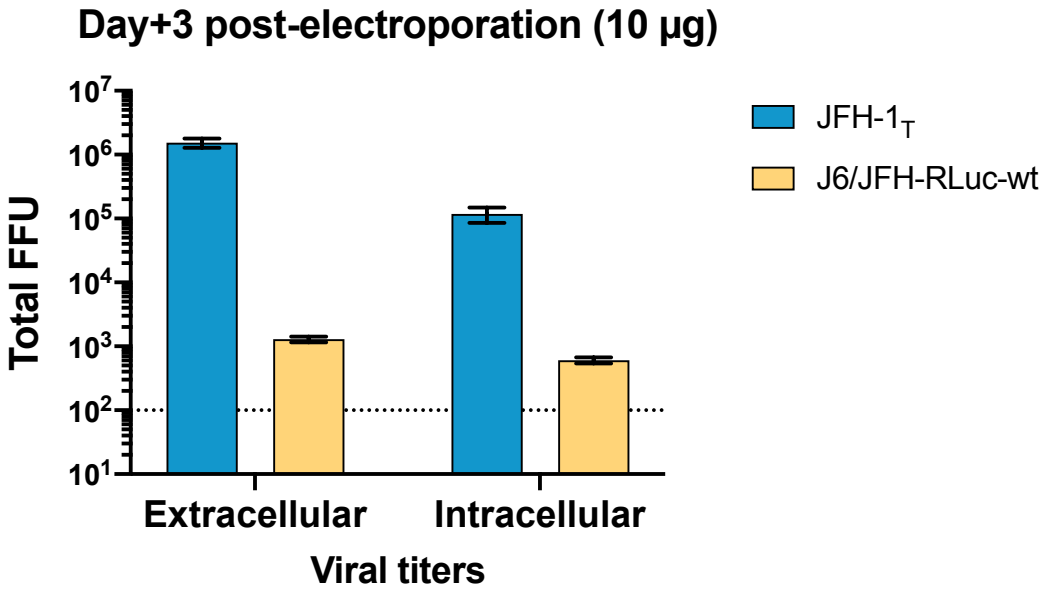

Supplementary Figure 2. The J6/JFH FL Rluc WT can produce infectious viral particles, but much less efficiently than JFH-1$_T$. Three days post-electroporation of viral RNA, intracellular and extracellular viral titers were harvested and assayed by focus-forming unit assay. Data is representative of one independent replicate measured in duplicate. The limit of detection is indicated (dotted line).